Formation of Paramagnetic Defect Centers in Aluminophosphate Molecular Sieves

Suk Bong Hong,* Sun Jin Kim, and Young Sun Uh*

Contribution from the Korea Institute of Science and Technology, P.O. Box 131, Cheongryang, Seoul 130-650, Korea

Received February 8, 1996[⊗]

Abstract: The formation of paramagnetic defect centers in aluminophosphate ($AlPO_4$) molecular sieves with different structures is investigated by electron spin resonance (ESR) spectroscopy. Distinct differences in the position and number of the ESR signals generated by dehydroxylation of $AlPO_4$ molecular sieves under a vacuum of 10^{-5} Torr at 773 K clearly show that the nature of the paramagnetic defect centers formed is significantly different in the structure type of the molecular sieves. In addition, it is found that the spin concentration of these defects depends strongly on the pore size of the $AlPO_4$ molecular sieves as well as their hydration level before dehydroxylation. The larger ring size the molecular sieve has, the higher spin concentration of paramagnetic defects it shows. Thus, the extra-large-pore VPI-5 shows the highest spin concentration value among the molecular sieves studied here, which corresponds to 6.4 defects per 1000 unit cells. The ESR results obtained from $AlPO_4$-based molecular sieves containing heteroatoms other than aluminum and phosphorus (such as silicon or cobalt) reveal that the formation of paramagnetic defect centers is severely restricted when the amount of heteroatoms in their framework increases. On the basis of the overall ESR results of this study, a reliable mechanism of formation of paramagnetic defect centers in $AlPO_4$ molecular sieves is proposed.

Introduction

The disclosure of aluminophosphate ($AlPO_4$) molecular sieves by scientists at Union Carbide Corp. in the early 1980s[1] has dramatically expanded the structural regime of crystalline microporous materials. To date, more than two dozen structure types of $AlPO_4$ molecular sieves have been reported. They not only include framework topologies related to those found in zeolites but also comprise a large number of novel structures; for example, the extra-large-pore VPI-5 (VFI topology) is a member of the $AlPO_4$ family.[2]

A serious drawback of $AlPO_4$ molecular sieves in terms of their applications as catalysts and separation media is the lack of Brønsted acid sites because of their neutral framework. Thus, considerable synthetic effort has been devoted to the generation of Brønsted acid sites in these materials by introducing heteroatoms other than aluminum and phosphorus, to produce negatively charged frameworks.[3−5] Hundreds of compositions of $AlPO_4$-based molecular sieves incorporating one or more of 13 elements from the periodic table have been prepared and include silicoaluminophosphates (SAPO) and metal-substituted aluminophosphates (MeAPO). Although these new classes of molecular sieves are known to be catalytically active for many chemical reactions, any simple relationship between Brønsted acidity and catalytic activity of the $AlPO_4$-based molecular sieves has not been found yet because their acidity is a complicated function of framework charge, structure type, and the nature of the element incorporated.[6]

An important, recurring question arising from the study of $AlPO_4$ molecular sieves is the unusual surface selectivity of $AlPO_4$ materials, which is significantly different from that of pure-silica molecular sieves or zeolites.[6,7] For example, their water sorption isotherms are characterized by the Brunauer type V isotherm which shows little initial adsorption at very low pressures followed by vertical rise in adsorption leading to complete fillings of pores.[7] In addition, previous studies on the *n*-hexane reactivity of platinum clusters supported on molecular sieves with the same framework structure but different compositions[8] revealed that the clusters on SSZ-24 show high selectivity to benzene with little formation of *n*-hexenes, while the opposite is observed for those on $AlPO_4$-5. Since the weight loading of platinum and H/Pt are almost the same for these two catalysts, the observed differences in the *n*-hexane reactivity are speculated to relate to the differences in the physicochemical properties of the molecular sieves used as platinum supports.[8] However, the precise reasons for the unusual surface selectivity of $AlPO_4$ molecular sieves are not completely understood. This suggests that there must be some intrinsic physicochemical properties of $AlPO_4$ materials which have remained elusive.

Many important properties of zeolites, most notably their ion exchange and catalytic properties, can be significantly influenced

* Author to whom correspondence should be addressed. Phone: +82-2-958-5088. Fax: +82-2-958-5089. E-mail: sbhong@kistmail.kist.re.kr or uhyoung@kistmail.kist.re.kr.

⊗ Abstract published in *Advance ACS Abstracts,* August 1, 1996.

(1) (a) Wilson, S. T.; Lok, B. M.; Messina, C. A.; Cannan, T. R.; Flanigen, E. M. *J. Am. Chem. Soc.* **1982**, *104*, 1146−1147. (b) Wilson, S. T.; Lok, B. M.; Flanigen, E. M. U.S. Patent 4 310 440, 1982.

(2) (a) Davis, M. E.; Saldarriaga, C.; Montes, C.; Garces, J.; Crowder, C. *Nature* **1988**, *331*, 698−699. (b) Li, H.-X.; Davis, M. E. *Catal. Today* **1994**, *19*, 61−106.

(3) (a) Flanigen, E. M.; Lok, B. M.; Patton, R. L.; Wilson, S. T. *Stud. Surf. Sci. Catal.* **1986**, *28*, 103−112. (b) Szostak, R. *Molecular Sieves: Principles of Synthesis and Identification*; Van Nostrand Reinhold: New York, 1989.

(4) (a) Lok, B. M.; Messina, C. A.; Patton, R. L.; Gajek, R. T.; Cannan, T. R.; Flanigen, E. M. U.S. Patent 4 440 871, 1984. (b) Lok, B. M.; Messina, C. A.; Patton, R. L.; Gajek, R. T.; Cannan, T. R.; Flanigen, E. M. *J. Am. Chem. Soc.* **1984**, *106*, 6092−6093.

(5) Lok, B. M.; Marcus, B. K.; Vail, L. D.; Flanigen, E. M.; Wilson, S. T. European Patent Application 159,624, 1985.

(6) Flanigen, E. M.; Patton, R. L.; Wilson, S. T. *Stud. Surf. Sci. Catal.* **1988**, *37*, 13−27.

(7) (a) Lohse, U.; Noack, M.; Jahn, E. *Adsorp. Sci. Technol.* **1986**, *3*, 19−24. (b) Thamm, H.; Stack, H.; Jahn, E.; Fahlke, B. *Adsorp. Sci. Technol.* **1986**, *3*, 217−220. (c) Malla, P. B.; Komarneni, S. *MRS Sym. Proc.* **1991**, *233*, 237−242.

(8) (a) Hong, S. B.; Mielczarski; Davis, M. E. *J. Catal.* **1992**, *134*, 349−358. (b) Mielczarski; Hong, S. B.; Davis, M. E. *J. Catal.* **1992**, *134*, 370−372.

S0002-7863(96)00419-2 CCC: $12.00

by the presence of structural defect sites in their framework.[9] Although there are extensive references on the nature of the defect sites in zeolites, little attention has been directed toward the characterization of structural defect sites in $AlPO_4$ molecular sieves and related materials. Very recently, we have demonstrated that the structural defects in $AlPO_4$ molecular sieves change into *paramagnetic* defect centers when dehydroxylated under a vacuum of 10^{-5} Torr at 773 K.[10] Also, we have shown that these centers can serve as effective electron donors for electron-withdrawing adsorbates such as O_2 and NO.

The purpose of this work is to elucidate the physicochemical properties of the $AlPO_4$ molecular sieves that are essential to produce paramagnetic defect centers via dehydroxylation. Here we present the electron spin resonance (ESR) spectra of dehydroxylated $AlPO_4$ molecular sieves which cover the range of crystallographically defined pore sizes from the small-pore (SOD) to the extra-large-pore (VFI) system. Also, the ESR spectra of dehydroxylated $AlPO_4$-based molecular sieves such as SAPO and CoAPO materials are reported. All the ESR results obtained here are used to propose a plausible mechanism of formation of paramagnetic defect centers in $AlPO_4$ molecular sieves.

Experimental Section

Sample Preparation. $AlPO_4$-5 was synthesized in accordance with the Union Carbide patent procedure.[1b] $AlPO_4$-5 was also synthesized in the presence of fluoride ions.[11] $AlPO_4$-11, $AlPO_4$-17, $AlPO_4$-18, and $AlPO_4$-20 were prepared according to the procedures described in the Union Carbide patent.[1b] VPI-5 was synthesized by the procedures given by Davis and Young.[12a] $AlPO_4$-8 was prepared by heating hydrated VPI-5 at 473 K for 24 h. $AlPO_4$ tridymite was synthesized according to the procedures described by Cheung *et al*.[12b] Amorphous $AlPO_4$ with Al/P = 1 was obtained by heating a layered $AlPO_4$ material in air at 873 K for 24 h, which was produced as an impurity during the preparation of $AlPO_4$-17. SAPO-5 and SAPO-37 were synthesized by the procedures given elsewhere.[4a,13] Two SAPO-34 molecular sieves in which the framework silicon contents are low and high, respectively, were prepared by varying the amount of the silicon source added during the crystallization.[4a] CoAPO-5 and CoAPO-34 were synthesized by the procedures described in the literature.[5] A proton form of ZSM-5 with a Si/Al ratio of 13.5 was obtained from ALSI-PENTA Zeolithe GmbH. Pure-silica ZSM-5 was synthesized by the method described in the literature.[14a] SSZ-24 was prepared by a modification of the Chevron patent.[14b] Structural information of all materials used in this study is given in Table 1.

Sample Treatments. All as-synthesized molecular sieves except VPI-5 and SAPO-37 were calcined in flowing O_2 at 823 K for 12−24 h to remove the organic structure-directing agents. As-synthesized VPI-5 was first evacuated at room temperature under vacuum to a residual pressure of 10^{-4} Torr overnight and then heated at 773 K for 2 h. The calcined samples were refluxed in water for 4 h and dried at room temperature. When necessary, the degree of hydration of calcined samples were adjusted by exposing them to ambient air at room temperature for different periods of time, without refluxing in water. Prior to ESR experiments, approximately 30 mg portions of the samples were placed into quartz tubes of 3-mm inner diameter, slowly heated in a vacuum of 10^{-5} Torr to 773 K, and then kept at this temperature for 2 h. As-synthesized SAPO-37 was heated in flowing O_2 at 823 K for 6 h, then evacuated under a vacuum of 10^{-5} Torr at this temperature for 2 h and cooled to 77 K to measure its ESR spectrum.

Table 1 Structural and Compositional Data of Molecular Sieves and Related Materials Used in This Study

sample	structure type	ring size	anhydrous unit cell composition	BET surface area[a] ($m^2\ g^{-1}$)
tridymite $AlPO_4$		6	$Al_2P_2O_8$	
$AlPO_4$-20	SOD	6	$Al_6P_6O_{24}$	
$AlPO_4$-17	ERI	8	$Al_8P_{18}O_{72}$	458
$AlPO_4$-18	AEI	8	$Al_{24}P_{24}O_{96}$	568
SAPO-34(I)	CHA	8	$Al_{18.0}P_{16.6}Si_{1.4}O_{72}$	604
SAPO-34(II)	CHA	8	$Al_{18.0}P_{15.8}Si_{2.2}O_{72}$	639
$AlPO_4$-11	AEL	10	$Al_{20}P_{20}O_{80}$	185
ZSM-5	MFI	10	$Al_{6.6}Si_{89.4}O_{192}$	431
$AlPO_4$-5	AFI	12	$Al_{12}P_{12}O_{48}$	337
SAPO-5	AFI	12	$Al_{11.3}P_{10.8}Si_{1.9}O_{48}$	302
CoAPO-5(I)	AFI	12	$Al_{11.9}P_{12.0}Co_{0.1}O_{48}$	331
CoAPO-5(II)	AFI	12	$Al_{11.0}P_{12.0}Co_{1.0}O_{48}$	329
SSZ-24	AFI	12	$Si_{24}O_{48}$	300
SAPO-37	FAU	12	$Al_{96}P_{72}Si_{24}O_{384}$	952
$AlPO_4$-8	AET	14	$Al_{36}P_{36}O_{144}$	62
VPI-5	VFI	18	$Al_{18}P_{18}O_{72}$	409
amorphous $AlPO_4$				14

[a] BET surface areas calculated from nitrogen adsorption data.

Analytical Methods. Crystallinity and phase purity of molecular sieves prepared here were determined by X-ray powder diffraction using a Rigaku D/Max-IIA diffractometer (Cu Kα radiation). All the materials are highly crystalline and no reflections other than those from each molecular sieve are observed. This can be further supported by the nitrogen BET surface area data (see Table 1), which were obtained on a Micromeritics ASAP 2000 analyzer. Elemental analysis for selected samples was performed by a Jarrell-Ash Polyscan 61E inductively coupled plasma (ICP) spectrometer in combination with a Perkin-Elmer 5000 atomic absorption spectrophotometer. The water contents of the samples refluxed in water followed by drying at room temperature were determined by a Dupont 950 thermogravimetric analyzer.

The ^{29}Si MAS NMR spectra of SAPO molecular sieves were recorded on a Bruker AM-300 FT-NMR spectrometer operating at a ^{29}Si frequency of 64.38 MHz. The samples were spun at 3.5 kHz and the spectra were obtained with an acquisition of *ca*. 5000 pulse transients, which was repeated with a 5-s recycle delay and 3-μs pulse width. The ^{29}Si chemical shifts are reported relative to TMS.

ESR measurements were performed at 77 K on a Bruker ER-200D spectrometer operating at X-band (≃9.45 GHz) with 100-kHz field modulation. The ESR spectra acquired were interfaced to a home-built signal average convertor and then transferred to an IBM compatible computer for storage, analysis, and plotting. The microwave frequency was monitored by an Anritsu MF76A microwave frequency counter to an accuracy of ±0.1 kHz, and g values were determined through comparison of the resonant field with that of the 2,2-diphenyl-1-picrylhydrazyl (DPPH) radical at $g = 2.0036$. The spin concentrations of the paramagnetic centers formed in dehydroxylated $AlPO_4$ molecular sieves and related materials were determined by comparing the intensities of the doubly integrated defect spectra with those obtained from various weighted amounts of copper(II) sulfate pentahydrate ($CuSO_4 \cdot 5H_2O$). The estimated error in spin concentration is ±50%. The ESR spectra were frequently contaminated by a sharp line at $g = 2.0035$ even after the prolonged thermal treatments of samples in flowing O_2 at temperatures higher than 823 K. This line is due to the residual carbonaceous materials produced during the calcination step. Thus, the ESR line at $g = 2.0035$ in the ESR spectra reported here has been eliminated for clarity.

Results and Discussion

ESR Results from $AlPO_4$ Molecular Sieves. Figure 1 shows the ESR spectra at 77 K developed after dehydroxylation of $AlPO_4$ molecular sieves with six different structures in a vacuum of 10^{-5} Torr at 773 K for 2 h. All the spectra in Figure

(9) Engelhardt, G.; Michel, D. *High-Resolution Solid-State NMR of Silicates and Zeolites*; Wiley: New York, 1987.

(10) (a) Hong, S. B.; Kim, S. J.; Uh, Y. S. *J. Phys. Chem*., in press. (b) Hong, S. B.; Kim, S. J.; Choi, Y. S.; Uh, Y. S. *Proceedings of the 11th International Zeolite Conference*; Chon, H., Ihm, S.-K., Uh, Y. S., Eds.; Elsevier: Amsterdam, in press.

(11) Guth, J. L.; Kessler, H.; Caullet, P.; Hazm, J.; Merrouche, A.; Patarin, J. *Proceedings of the 9th International Zeolite Conference*; von Ballmoos, R., Higgins, J. B., Treacy, M. M. J., Eds.; Butterworth-Heinemann: Stoneham, MA, 1993; Vol. 1, p 215.

(12) (a) Davis, M. E.; Young, D. *Stud. Surf. Catal*. **1991**, *60*, 53−62. (b) Cheung, T. T. P.; Willcox, K. W.; McDaniel, M. P.; Johnson, M. M. *J. Catal*. **1986**, *102*, 10−20.

(13) Sierra de Saldarriaga, L.; Saldarriaga, C.; Davis, M. E. *J. Am. Chem. Soc*. **1987**, *109*, 2686−2691.

(14) (a) Szostak, R. *Handbook of Molecular Sieves*; Van Nostrand Reinhold: New York, 1992. (b) Zones, S. I. U.S. Patent 4 665 110, 1987.

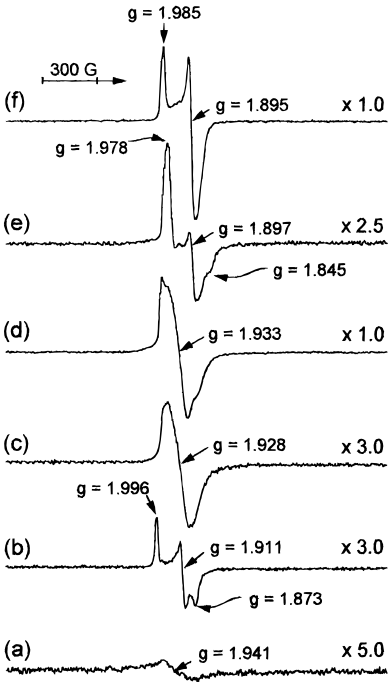

Figure 1. ESR spectra at 77 K of paramagnetic defect centers formed in $AlPO_4$ molecular sieves with different structures: (a) $AlPO_4$-20, (b) $AlPO_4$-17, (c) $AlPO_4$-11, (d) $AlPO_4$-5, (e) $AlPO_4$-8, and (f) VPI-5. Prior to ESR measurements, all samples were first refluxed in water for 4 h and then dehydroxylated under a vacuum of 10^{-5} Torr at 773 K for 2 h.

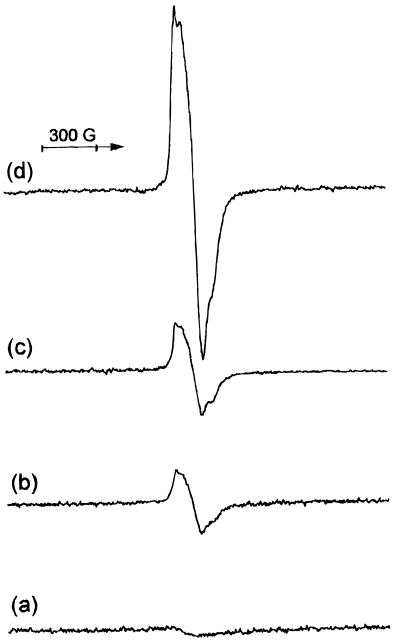

Figure 2. ESR spectra at 77 K of paramagnetic defect centers developed after dehydroxylation of $AlPO_4$-5 samples with different hydration levels. As-synthesized $AlPO_4$-5 was first calcined in flowing O_2 at 823 K for 12 h and then transferred to an ESR tube (a) without exposure to atmospheric moisture, (b) after rehydration in air for 3 d, (c) after rehydration in air for 5 d, and (d) after refluxing in water for 4 h. The dehydroxylation conditions used are the same as those in Figure 1.

1 were obtained from the $AlPO_4$ molecular sieves refluxed in water for 4 h before dehydroxylation, in order to maximize their ESR signal intensities (*vide infra*). The hydrated $AlPO_4$ molecular sieves exhibited no ESR signals. As seen in Figure 1, however, distinct ESR signals were produced when they were dehydroxylated under conditions described above. Numerous papers on the characterization of paramagnetic defect centers in zeolites have involved the samples exchanged with various metal cations. In the majority of cases, paramagnetic defect centers are formed by γ or X irradiation of the zeolites after their dehydroxylation at high temperatures.[15] However, it is also reported that the formation of paramagnetic defect centers in zeolites can be achieved only by dehydroxylation, if the zeolites contain no metal cations.[16] Actual $AlPO_4$ molecular sieve crystals cannot be crystallographically perfect because of the structural defects generated during the synthesis and postsynthesis treatments. In addition, they have no charge-balancing metal cations due to their neutral framework. Therefore, we speculate that the ESR signals shown in Figure 1 are attributed to the paramagnetic centers, which were generated by dehydroxylation of the structural defects in hydrated $AlPO_4$ molecular sieves.

One may speculate that the reason $AlPO_4$ molecular sieves show ESR signals after dehydroxylation is that the materials prepared here contain a small amount of paramagnetic impurities such as transition metal ions, which possibly originated from the chemicals used in their synthesis. To rule out this possibility, we have performed ESR measurements on a series of $AlPO_4$-5 samples with different levels of hydration. Figure 2 shows the ESR spectra at 77 K developed after dehydroxylation of $AlPO_4$-5 samples in differently hydrated states. Figure 2a was obtained from the sample which was not exposed to atmospheric moisture after its calcination for the elimination of the occluded organic structure-directing agent. This spectrum shows a very weak ESR signal at $g = 1.933$. Interestingly, the intensity of this signal becomes stronger with increase of the hydration level of $AlPO_4$-5 before its dehydroxylation. Eventually, the strongest signal intensity is observed from $AlPO_4$-5 refluxed in water for 4 h, as seen in Figure 2d. The ESR signal from this $AlPO_4$-5 sample is approximately 2 orders of magnitude stronger than that in Figure 2a. It is expected that the amounts of paramagnetic impurities possibly present in $AlPO_4$-5 samples with different levels of hydration would not be significantly different, since essentially the same amount of solids has been used in obtaining the spectra in Figure 2. Thus, if $AlPO_4$-5 used here is contaminated by paramagnetic impurities, the ESR intensity should not be remarkably changed with the hydration level of $AlPO_4$-5 prior to dehydroxylation. The other structure types of $AlPO_4$ molecular sieves with different levels of hydration also show the same changes in ESR signal intensity as those found in Figure 2. This argument taken in total led us to believe that all the ESR signals in Figure 1 are attributed to the paramagnetic defect centers formed in $AlPO_4$ molecular sieves. It is interesting to note that a six-line hyperfine structure with a splitting of approximately 38 G is observable in Figure 2d, although it is not well-resolved. This can be attributed to an unpaired electron trapped on defect centers, where it interacts with one aluminum atom ($I = 5/2$) of the $AlPO_4$-5 framework.[10a]

Two important results are observed in the ESR spectra shown in Figure 1. First, the position and number of the ESR signals in these spectra differ significantly according to the structure type of the molecular sieves. For example, $AlPO_4$-5 shows a broad signal centered at $g = 1.933$. However, VPI-5 exhibits two signals which appear at $g = 1.985$ and 1.895. On the other hand, the ESR spectrum obtained from $AlPO_4$-17 is characterized by three signals at $g = 1.996$, 1.911, and 1.873. Second, the relative intensities of the ESR signals become stronger when the pore size of an $AlPO_4$ molecular sieve is larger. Thus, VPI-5 with 18-membered rings gives ESR signals which are stronger

(15) (a) Che, M.; Tench, A. J. *Adv. Catal.* **1983**, *32*, 1−148. (b) Lunsford, J. H. *Adv. Catal.* **1972**, *22*, 265−344.

(16) (a) Shih, S. *J. Catal.* **1983**, *79*, 390−395. (b) Ryoo, R.; Ihee, H.; Kwak, J. H.; Seo, G.; Liu, S. B. *Microporus Mater.* **1995**, *4*, 59−64.

Table 2. Spin Concentrations of Paramagnetic Defects Formed in Dehydroxylated $AlPO_4$ Molecular Sieves and Related Materials

sample	pore size (Å)	spin concentration[a] (10^{17} g^{-1})	no. of paramagnetic defect centers per 1000 unit cells
$AlPO_4$ tridymite		0.4	<0.1
$AlPO_4$-20	2.2	1.1	0.1
$AlPO_4$-17	3.1 × 5.1	2.8	1.0
$AlPO_4$-18	3.8	0.6	0.3
SAPO-34(I)	3.8	0.5	0.2
$AlPO_4$-11	3.9 × 6.3	4.9	2.0
$AlPO_4$-5	7.3	16.3	4.0
$AlPO_4$-5[b]	7.3	0.9	0.2
SAPO-5	7.3	3.9	1.0
CoAPO-5(I)	7.3	6.3	1.5
$AlPO_4$-8	7.9 × 8.7	7.7	5.6
VPI-5	12.1	17.5	6.4
amorphous $AlPO_4$		0.3	

[a] Determined by comparing the intensities of the doubly integrated defect spectra with those obtained from various weighted amounts of $CuSO_4 \cdot 5H_2O$. The estimated error in spin concentration is ±50%. [b] Prepared in the presence of F^- ions.

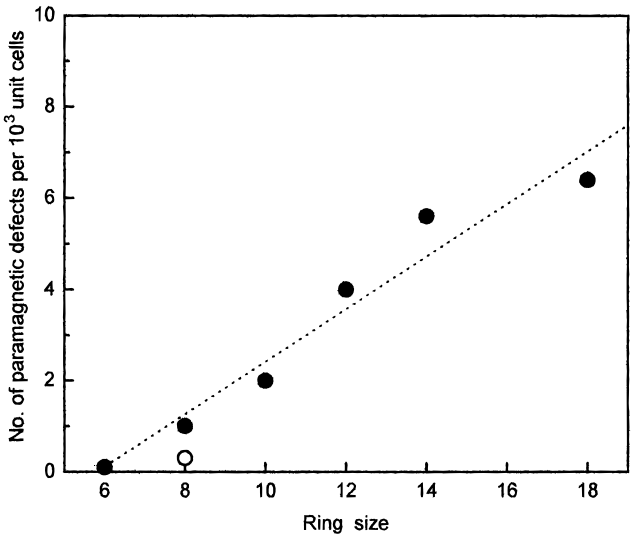

Figure 3. Plot of the number of paramagnetic defects per unit cell versus the T-atom number of the largest rings in $AlPO_4$ molecular sieves. The open circle indicates the number of paramagnetic defects per unit cell obtained from $AlPO_4$-18.

than those from any other molecular sieve studied here. This observation suggests that the amount of paramagnetic defect centers depends on the pore size of the $AlPO_4$ molecular sieves (*vide infra*). Upon exposure to 10 Torr of oxygen, all the signals in the ESR spectra of Figure 1 are immediately destroyed, but the O_2^- ESR signals have been produced.[10b] Therefore, it is most likely that the structural defects in dehydroxylated $AlPO_4$ molecular sieves would trap electrons to produce the F-type centers. We speculate that the observed differences in the position and number of the ESR signals in Figure 1 are due to the formation of different types of F centers, depending on the structure type of the molecular sieves, although it is not possible to make an unequivocal identification of these F-type centers. The aluminum and phosphorus atoms in $AlPO_4$ molecular sieves occupy tetrahedral framework positions in strict alteration with Al/P = 1. However, the tetrahedral atom sites are crystallographically different in the structure type of the molecular sieves. Furthermore, several different tetrahedral atom sites can exist in a particular structure type. This suggests that there must be crystallographic differences in the tetrahedral framework atoms which are part of the paramagnetic defect centers. From this point, we believe that the local environment of electrons trapped on the paramagnetic defect centers can differ according to the structure type of the $AlPO_4$ molecular sieves, which causes differences in the position and number of the observed ESR signals. On the other hand, all the ESR signals in Figure 1 disappeared when dehydroxylated $AlPO_4$ materials were exposed to water vapor. However, these signals were regenerated when hydrated $AlPO_4$ molecular sieves were dehydroxylated under conditions described earlier. Therefore, it is most likely that the formation of paramagnetic centers in $AlPO_4$ molecular sieves is reversible.

The spin concentrations of the paramagnetic defects formed in a variety of $AlPO_4$ molecular sieves and related materials are listed in Table 2. These data reveal that, among the molecular sieves studied here, the extra-large-pore VPI-5 shows the largest spin concentration value (*ca.* 1.8×10^{18} g^{-1}). This material was calculated to contain 6.4 defects per 1000 unit cells. Table 2 also reveals that paramagnetic defect centers can be generated on nonmicroporous $AlPO_4$ materials such as tridymite and amorphous phases, although their amounts are small as compared to those from $AlPO_4$ molecular sieves. For example, the ESR spectrum (not shown) of dehydroxylated amorphous $AlPO_4$ (Al/P = 1) is characterized by a weak, broad signal at $g = 1.946$. The amorphous $AlPO_4$ phase has a surface area of approximately 14 m^2 g^{-1}. Thus, the presence of an $AlPO_4$ molecular sieve may not be necessary. However, microporosity may play a significant role in achieving high concentrations of paramagnetic defects. From the anhydrous unit cell weights of the $AlPO_4$ molecular sieves, the numbers of paramagnetic defects per 1000 unit cells can be calculated and are also listed in Table 2. Notice that the larger pore size the dehydroxylated molecular sieve has, the more defects per 1000 unit cells are generated. In order to develop a more quantitative version of this correlation, we have focused on the number of tetrahedral atoms in the largest rings of each $AlPO_4$ molecular sieve as a structural parameter. As seen in Figure 3, there is a nearly linear relationship between the number of paramagnetic defects per 1000 unit cells and the T-atom number of the largest rings present in each $AlPO_4$ molecular sieve, with the exception of $AlPO_4$-18. To the best of our knowledge, this is the first study showing that the amount of paramagnetic defects in molecular sieves is dependent on the size of the largest rings present in molecular sieves.

The structural defects in $AlPO_4$ molecular sieves can be simply depicted as either T−O^- or T−OH groups, where T is aluminum or phosphorus. The type and amount of structural defects in zeolites are known to depend on a number of factors including synthesis method,[17] framework composition[18] and the manner of sample treatment.[19] $AlPO_4$ molecular sieves and related materials are usually prepared in the absence of inorganic cations. Thus, the T−O^- defects in an as-synthesized form of these molecular sieves balance primarily the charge of organic cations present in their cavities. On the other hand, T−OH groups exist on the external surface of the crystals and can be generated by hydrolysis of T−O−T linkages, removal of

(17) (a) Chezeau, J. M.; Delmotte, L.; Guth, G. L.; Soulard, M. *Zeolites* **1989**, *9*, 78−80. (b) Axon, S. A.; Klinowski, J. *Appl. Catal.* **1992**, *81*, 27−34. (c) Vinje, K.; Ulan, J.; Szostak, R.; Gronsky, R. *Appl. Catal.* **1991**, *72*, 361−372. (d) Annen, M. J.; Young, D.; Davis, M. E.; Cavin, O. B.; Hubbard, C. R. *J. Phys. Chem.* **1991**, *95*, 1380−1383. (e) He, H.; Barr, T. L.; Klinowski, J. *J. Phys. Chem.* **1994**, *98*, 8775−8779. (f) Koller, H.; Lobo, R. F.; Burkett, S. L.; Davis, M. E. *J. Phys. Chem.* **1995**, *99*, 12588−12596.

(18) (a) Chester, A. W.; Chu, Y. F.; Dessau, R. M.; Kerr, G. T.; Kresge, C. T. *J. Chem. Soc., Chem. Commun.* **1985**, 289−290. (b) Woolery, G. L.; Alemany, L. B.; Dessau, R. M.; Chester, A. W. *Zeolites* **1986**, *6*, 14−16.

(19) (a) Engelhardt, G.; Fahlke, B.; Magi, M.; Lippmaa, E. *Z. Phys. Chem. (Leipzig)* **1985**, *266*, 239−245. (b) Fyfe, C. A.; Gobbi, G. C.; Kennedy, G. J. *J. Phys. Chem.* **1984**, *88*, 3248−3253. (c) Samoson, A.; Lippmaa, E.; Engelhardt, G.; Lohse, U.; Jerschkewitz, H. G. *Chem. Phys. Lett.* **1987**, *134*, 589−592.

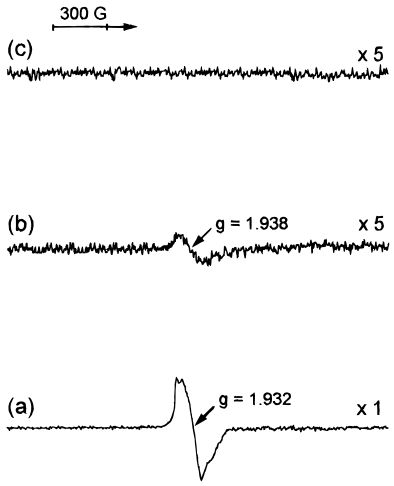

Figure 4. ESR spectra at 77 K of dehydroxylated (a) SAPO-5, (b) SAPO-34(I), and (c) SAPO-34(II) molecular sieves. The ESR signal intensity is referenced relative to the signal in Figure 2d. The dehydroxylation conditions used are the same as those in Figure 1.

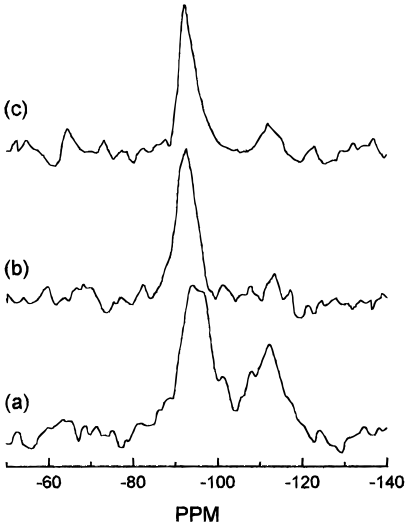

Figure 5. ^{29}Si MAS NMR spectra of as-synthesized (a) SAPO-5, (b) SAPO-34(I) and (c) SAPO-34(II) molecular sieves.

tetrahedral framework atoms, or stacking disorder. Recently, Parlitz *et al.*[20] have reported that some Al−O−P linkages in $AlPO_4$ molecular sieves can be hydrolyzed by the adsorption of water in the temperature region between 323 and 473 K, leading to an increase in the amount of Al−OH and P−OH groups. If the formation of paramagnetic defect centers in $AlPO_4$ molecular sieves during the dehydroxylation step occurs mainly in the defects generated by hydrolysis of Al−O−P linkages, their ESR signal intensity should not differ significantly according to the method of molecular sieve synthesis. In order to test whether this speculation is correct, we have prepared $AlPO_4$-5 in the presence of fluoride anions and performed ESR measurements on this $AlPO_4$-5 sample. Although this sample was calcined and then refluxed in water before dehydroxylation, the observed intensity of its ESR signal was found to be much weaker than that in Figure 2d. This is not unexpected because the use of F^- ions as mineralizing agents in the synthesis of zeolites is known to significantly reduce the amount of structural defects.[17a,b] Therefore, it is most likely that the amount of $T-O^-$ defects in $AlPO_4$-5 prepared in the presence of F^- ions must be very small as compared to that of $T-O^-$ defects in $AlPO_4$-5 prepared by the conventional method. This suggests that the formation of paramagnetic defect centers in $AlPO_4$ molecular sieves may be associated with the $T-O^-$ defects generated during the synthesis rather than with T−OH groups derived from hydrolysis of Al−O−P linkages or those present on the external surface of the crystals. As shown in Figure 2, however, there is a strong dependence on the hydration level of $AlPO_4$ molecular sieves before dehydroxylation for the intensities of the ESR signals from paramagnetic defect centers. This result can be rationalized by suggesting that $T-O^-$ defects in calcined $AlPO_4$ molecular sieves should be transformed into T−OH groups via hydration in order to form paramagnetic defect centers by subsequent dehydroxylation. A plausible mechanism of formation of paramagnetic defect center in $AlPO_4$ molecular sieves will be given below.

ESR Results from $AlPO_4$-Based Molecular Sieves. Figure 4 shows the ESR spectra recorded at 77 K after dehydroxylation of SAPO-5, SAPO-34(I), and SAPO-34(II) under conditions described earlier. Figure 4a was obtained from SAPO-5 (Si/Al = 0.17), which exhibits essentially the same position and shape as those of the signal from $AlPO_4$-5. However, notice that the relative intensity of this signal is approximately one-third of that in Figure 2d. This indicates that the substitution of silicon into the $AlPO_4$-5 framework results in a decrease in the amount of paramagnetic defects. It is well-established that the silicon substitution into the framework of $AlPO_4$ molecular sieves can be for phosphorus, an aluminum−phosphorus pair, or both of them.[13,21] As seen in Figure 5a, the ^{29}Si MAS NMR spectrum of SAPO-5 used here shows two broad resonances at −95 and −115 ppm. Thus, the silicon atoms in our SAPO-5 substitute for a portion of phorphorus atoms and Al−O−P linkages. This indicates that this SAPO-5 sample includes three distinct regions with different oxide compositions: aluminophosphate, silicoaluminophosphate, and silica. Structural defects can exist in all three regions. However, those in the silica region do not appear to be involved in the formation of paramagnetic defect centers. This is because SSZ-24, which is the pure silica form of $AlPO_4$-5, shows no noticeable ESR signal even after dehydroxylation under more severe conditions than those described earlier. Then, it is interesting to examine whether paramagnetic defect centers can be generated in the silicoaluminophosphate region where silicon, aluminum, and phosphorus atoms are homogeneously distributed. This can be unravelled by ESR measurements on SAPO-34 molecular sieves with low and high silicon contents. These two SAPO-34 samples show only one narrow resonance around −92 ppm, as seen in parts b and c of Figure 5. Thus, they contain only one type of silicon environment, i.e., Si(4Al). This implies that we can eliminate any ambiguity arising from multiple silicon environments in the interpretation of the ESR results from these SAPO-34 samples. Figure 4b was obtained after dehydroxylation of SAPO-34(I) with a Si/Al ratio of 0.08. The spectrum is characterized by a very weak signal at $g = 1.938$, which indicates the presence of paramagnetic centers. However, no detectable ESR signals are observed in Figure 4c obtained from SAPO-34(II) with a higher Si/Al ratio (0.12). Therefore, it is most likely that the substitution of phosphorus by silicon in the hypothetical $AlPO_4$-34 framework reduces significantly the amount of paramagnetic defect centers.

To more accurately ensure the conclusion given above, we have also measured the ESR spectrum of SAPO-37. The tetrahedral (T) atom ratios of SAPO-37 prepared in this study was found to be 4:3:1 Al:P:Si within experimental error (see Table 1). In addition, the ^{29}Si MAS NMR spectrum (not shown) of SAPO-37 gives only one narrow resonance at −90 ppm.

(20) Parlitz, B.; Lohse, U.; Schreier, E. *Microporous Mater*. **1994**, *2*, 223−228.

(21) Hasha, D.; Sierra de Saldarriaga, L.; Saldarriaga, C.; Hathaway, P. E.; Cox, D. F.; Davis, M. E. *J. Am. Chem. Soc.* **1988**, *110*, 2127−2135.

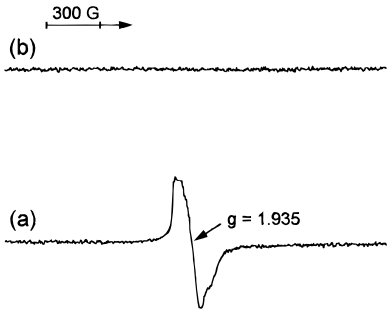

Figure 6. ESR spectra at 77 K of dehydroxylated CoAPO-5 molecular sieves with low and high Co contents: (a) CoAPO-5(I) and (b) CoAPO-5(II). The ESR signal intensity is referenced relative to the signal in Figure 2d. The dehydroxylation conditions used are the same as those in Figure 1.

These results indicate a homogeneous distribution of silicon, aluminum, and phosphorus atoms in the SAPO-37 framework. Unfortunately, the structure of SAPO-37 after removal of the occluded organic structure-directing agents collapses completely during the rehydration step at room temperature because of its poor resistance to water. Thus, ESR measurements on SAPO-37 have been performed without rehydration after calcination of the as-synthesized sample. No noticeable ESR signals are observed. The same result was also obtained from the amorphous SAPO phase, which was prepared by refluxing calcined SAPO-37 in water for 4 h. As described earlier, however, amorphous $AlPO_4$ with Al/P = 1 shows a weak, broad ESR signal at $g = 1.946$. Therefore, it appears that the formation of paramagnetic centers in SAPO molecular sieves is not possible in the silicoaluminophosphate region.

Let us now attempt to investigate whether the substitution of aluminum by heteroatoms in the $AlPO_4$ framework affects the formation of paramagnetic defect centers. Figure 6 shows the ESR spectra at 77 K of two CoAPO-5 samples with different cobalt contents. CoAPO-5(I) with a very low Co/P ratio (0.01) shows a broad ESR signal at $g = 1.933$. Notice that the position and shape of this signal are quite similar to those of the signal from $AlPO_4$-5, but its intensity is less than a half of that in Figure 2d. On the other hand, no detectable ESR signals are observed from CoAPO-5(II) with a Co/P ratio of 0.08, indicating the absence of paramagnetic defect centers. Unlike the SAPO molecular sieves described above, cobalt in CoAPO-5 samples substitutes exclusively for aluminum. Therefore, it appears that the cobaltophosphate region in CoAPO-5, produced by substitution of cobalt for aluminum, would not be involved in the formation of paramagnetic defect centers. The chemical composition data in Table 1 show that cobalt in CoAPO-5(II) has replaced only a small portion of the framework aluminum atoms. This indicates that the cobaltophosphate region in this CoAPO-5 sample is much smaller than the aluminophosphate region. It is reported that the amount of internal Si−OH defects in ZSM-5 decreases significantly with increasing aluminum content in the zeolite.[18b] Therefore, we cannot rule out the possibility that, regardless of the type of heteroatoms substitution, an increase in the content of heteroatoms other than aluminum and phosphorus in the framework of the $AlPO_4$-based molecular sieves leads to a significant decrease in the number of the inherently structural defects which can be transformed into paramagnetic defect centers during the dehydroxylation step.

Mechanism of Paramagnetic Defect Center Formation in $AlPO_4$ Molecular Sieves. Unlike zeolites, the $AlPO_4$ molecular sieves are built from alternating AlO_4^- and PO_4^+ tetrahedra. Thus, the local aluminum and phosphorus environments present in their structural defects can be expressed as $Al(OH)_n(OP)_{4-n}$ and $P(OH)_n(OAl)_{4-n}$ with $n = 1-4$, respectively. This implies that the presence of hydroxyl nests generated by missing

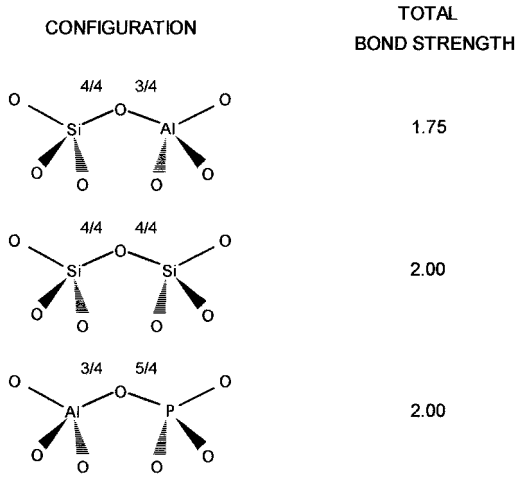

Figure 7. Bond strengths on bridging oxygen atoms in zeolites and pure-silica and $AlPO_4$ molecular sieves.

Scheme 1

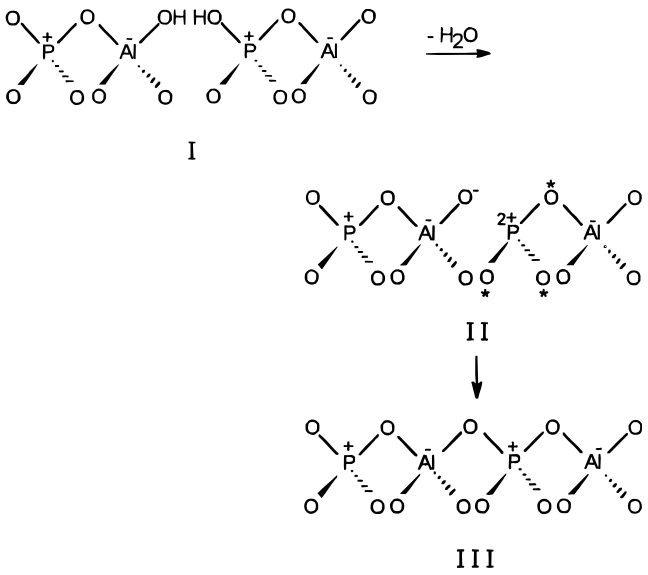

tetrahedral framework atoms (T vacancies) is also possible. According to Pauling's bonding rules,[22] on the other hand, the bond strength on the bridging oxygen atoms in a perfect molecular sieve framework should not exceed their valency, i.e., 2. In Figure 7 this principle is illustrated for zeolites and pure-silica and $AlPO_4$ molecular sieves. The ESR results obtained from this study demonstrate that paramagnetic defect centers are easily formed in $AlPO_4$ molecular sieves after dehydroxylation of the molecular sieves under a vacuum of 10^{-5} Torr at 773 K. This suggests that not all bridging oxygen atoms can reside in dehydroxylated molecular sieves, without violating bond strength concepts. Therefore, we have investigated bond strengths on bridging oxygen atoms in possible defect structures after dehydroxylation. For convenience sake, the defect structure considered here is postulated to contain two hydroxyl groups attached to adjacent aluminum and phosphorus that are part of the $AlPO_4$ molecular sieve framework, as seen in structure **I** of Scheme 1. The dehydroxylation process in this defect structure can occur between (1) the proton of hydroxyl attached to aluminum and the hydroxyl linked into phorphorus or (2) the hydroxyl attached to aluminum and the proton of hydroxyl linked into phosphorus. If mechanism 1 is dominant, dehydroxylation may proceed via the breaking of one P−O bond instead of one Al−O bond. Then, phosphorus would be

(22) (a) Pauling, L. *J. Am. Chem. Soc.* **1929**, *51*, 1010−1026. (b) Davis, M. E. *Acc. Chem. Res.* **1993**, *26*, 111−115.

Scheme 2

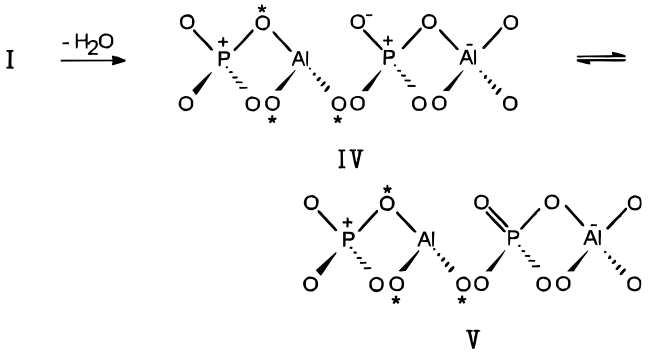

surrounded by three bridging oxygen atoms with a bond strength of 3/4 + 5/3 = 2.42, as indicated by an asterisk in structure **II**. However, mechanism 1 yields one Al−O bond where both aluminum and oxygen atoms have a single negative charge. As a result, structure **II** is unlikely to exist and structural rearrangement may occur via the P−O bond formation. This produces the perfect framework (structure **III**), implying that the formation of paramagnetic defect centers cannot be followed by mechanism 1. This speculation can be further supported by the fact that the enthalpy (*ca*. 143 kcal mol^{-1}) of the P−O bond dissociation is higher than that (*ca*. 122 kcal mol^{-1}) of the Al−O bond dissociation. On the other hand, if mechanism 2 occurs, then structure **IV** would be observed (Scheme 2).

Unlike structure **II**, this structure has no contradiction concerning the charge distribution, since it contains one P−O bond where phosphorus and oxygen have a single positive charge and a single negative charge, respectively. Also, it is expected that structure **IV** be transformed into a more stable structure **V** containing one P═O bond. Notice that the bond strength (3/3 + 5/4 = 2.25) on bridging oxygen atoms linked into the tricoordinated aluminum of structure **IV** or **V** is weaker than that (3/4 + 5/3 = 2.42) of oxygen atoms linked into the tricoordinated phosphorus of structure **II**, but it is still higher than 2. Therefore, it is most likely that the formation of paramagnetic defect centers in $AlPO_4$ molecular sieves may proceed via mechanism 2 rather than mechanism 1. If such is the case, where does the paramagnetism come from? As demonstrated in Figure 1, no strong hyperfine interactions between the unpaired electron and the tricoordinated aluminum atom (I = 5/2) in the $AlPO_4$ framework were found. This suggests that the paramagnetism is not due to the tricoordinated aluminum in structure **IV** or **V**.[10a] Thus, we speculate that it originates largely from bridging oxygen atoms linked into the tricoordinated aluminum. This speculation can be further supported by the fact that the ESR spectra of O_2^- generated in dehydroxylated $AlPO_4$ molecular sieves with different structures by adsorption of O_2 show no hyperfine splittings, although they have been taken even at a very low temperature, i.e., 4 K.[10b]

Dehydroxylation of Zeolites and Pure-Silica Molecular Sieves. As described earlier, the production of paramagnetic defect centers in zeolites normally requires dehydroxylation of the zeolites at high temperatures and subsequent γ or X irradiation.[15] However, there are several examples where irradiation is not necessary to produce paramagnetic centers.[15,23] In such cases, dehydroxylation is sufficient because the extraframework metal cations balancing the negative framework charges of zeolites or present as impurities in zeolites can act as paramagnetic centers. On the other hand, the production of paramagnetic defects in decationated zeolites without irradiation is rare but known. For example, Shih[16a] has observed an ESR signal at g = 2.0028 from H-ZSM-5 (Si/Al = 22) calcined in flowing O_2 at 773 K. He has proposed that high-temperature calcination of H-ZSM-5 under the flow of O_2 or air gives rise to the formation of paramagnetic defect centers via the chemical reaction outlined in Scheme 3. Thus, the paramagnetic defect

Scheme 3

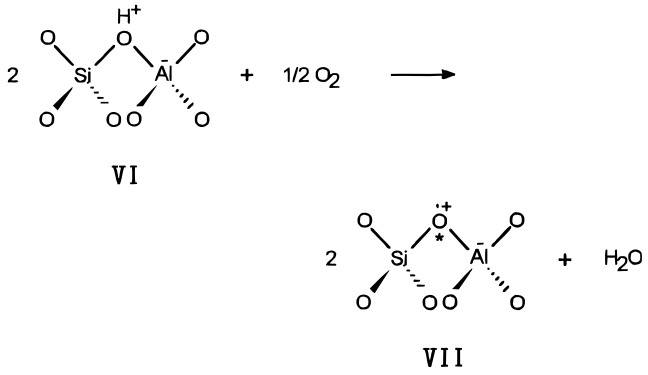

centers generated have been attributed to positive holes (V centers) on bridging oxygen atoms in Brønsted acid sites. This speculation can be further supported by the fact that the ESR signal at g = 2.0028 due to paramagnetic defects in H-ZSM-5 is not destroyed by exposure to O_2,[16] unlike the signals from $AlPO_4$ materials. However, the reaction in Scheme 3 reveals that the formation of paramagnetic defect centes in H-ZSM-5 requires the dehydroxylation of the zeolite in the presence of O_2. This suggests that the formation of paramagnetic defect centers in decationated zeolites is not possible when the zeolites are dehydroxylated under the conditions used in this study, i.e., in the absence of O_2. We have performed ESR measurements on H-ZSM-5 (Si/Al = 13.5), which had been pretreated under a vacuum of 10^{-5} Torr from room temperature to 773 K and kept at this temperature for another 2 h. As expected, no detectable ESR signals are observed. To rationalize this observation, we start by considering a possible dehydroxylation pathway in ideally defect-free, decationated zeolites. This is because they contain no extraframework metal cations that can serve as paramagnetic centers. As seen in structure **VIII** of Scheme 4, the ideally protonated form contains hydroxyls which are protons associated with negatively charged framework oxygens linked into AlO_4^- tetrahedra (Brønsted acid sites). The protons are very mobile at temperatures higher than 473 K and

Scheme 4

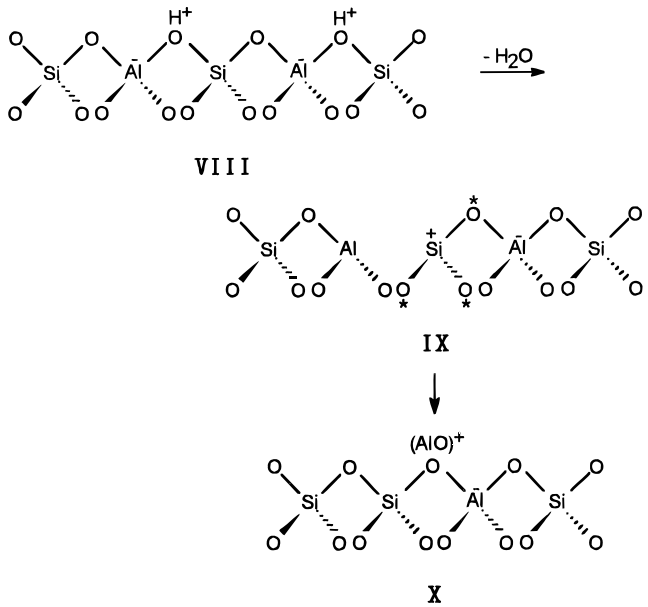

(23) Imai, T.; Habgood, H. W. *J. Phys. Chem.* **1973**, *77*, 925−931.

are thus lost as water with the consequent formation of Lewis acid sites (structure **IX**). Bridging oxygen atoms adjacent to the tricoordinated silicon in structure **IX** possess the bond strength of 3/4 + 4/3 = 2.08. However, structure **IX** should not be stable since the tricoordinated silicon is positively charged.[24] Consequently, an annealing process may stabilize the structure and produce the so-called "true" Lewis acid sites (structure **X**) by ejecting aluminum from the framework. Therefore, it is most likely that the dehydroxylation of defect-free, decationated zeolites under a high vacuum or in the absence of O_2 does not lead to the formation of paramagnetic defect centers, although their formation as unstable, short-lived transition states cannot be ruled out.

A logical next step would be to consider the dehydroxylation in decationated but defect-containing zeolites. For convenience sake, the defect structure in these zeolites is assumed to contain two hydroxyls attached to adjacent aluminum and silicon atoms, as shown in structure **XI** of Scheme 5. Thus, the dehydroxylation process in this structure can take place between (1) the proton of hydroxyl attached to aluminum and the hydroxyl linked to silicon, and *vice versa*, (2) the proton of Brønsted acid sites and the hydroxyl attached to either aluminum or silicon, or (3) the hydroxyl of Brønsted acid sites and the proton of hydroxyl linked into either aluminum or silicon. If dehydroxylation mechanism 1 is dominant, Brønsted acid sites (structure **VIII**) should be created. Then, it is expected that further dehydroxylation may proceed via the pathway analogous to that stated in ideally defect-free, decationated zeolites (see Scheme 4). The same result is observed from dehydroxylation via mechanism 2 or 3 (see Schemes 6 and 7). This is because

Scheme 5

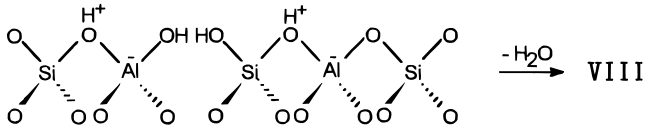

XI

Scheme 6

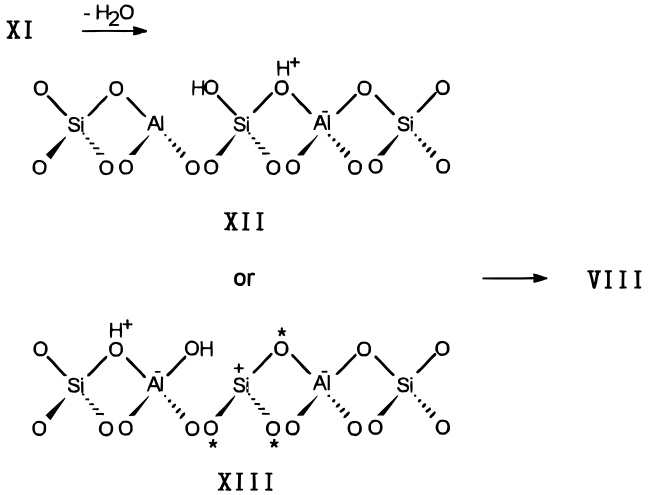

the Al−O bond formation (*ca.* −122 kcal mol^{-1}) or the Si−O bond formation (*ca.* −191 kcal mol^{-1}) in structures **XII**−**XV** is more thermodynamically favorable than the O−H bond formation (*ca.* −102 kcal mol^{-1}). Therefore, it can be concluded from Schemes 4−7 that dehydroxylation *in vacuo*

(24) Dyer, A. *An Introduction to Zeolite Molecular Sieves*; Wiley: New York, 1988.

Scheme 7

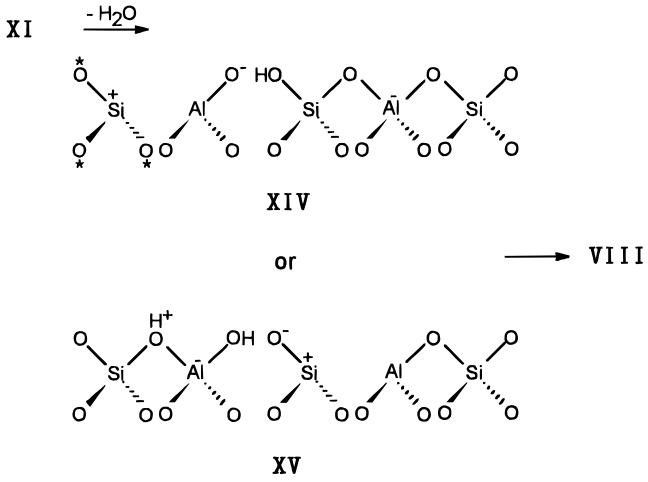

of decationated zeolites at high temperatures does not lead to the formation of paramagnetic centers, regardless of the presence of structural defects.

Finally, we discuss dehydroxylation in pure-silica molecular sieves containing structural defects. As seen in structure **XVII** of Scheme 8, dehydroxylation in these molecular sieves may

Scheme 8

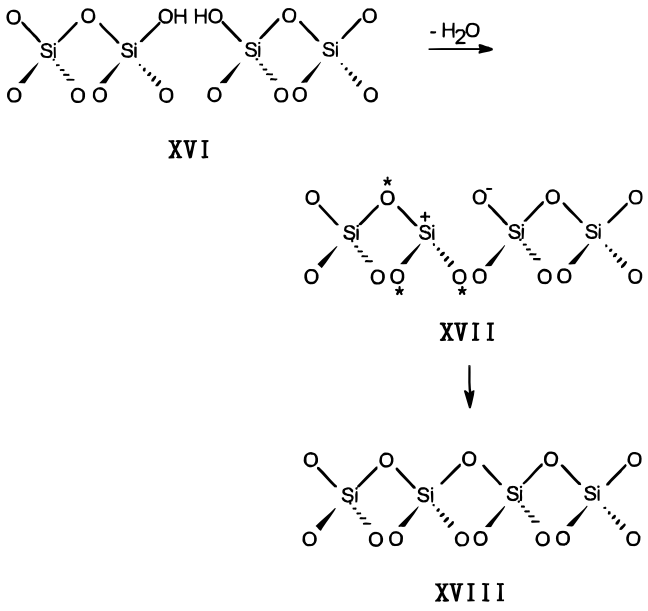

yield the formation of a positively charged, tricoordinated silicon. Furthermore, a Si−O$^-$ group must be adjacent to tricoordinated silicon in this structure. Thus, structure **XVII** is unlikely to exist and the perfect framework (structure **XVIII**) would be produced via one Si−O bond formation. This suggests that paramagnetic defect centers cannot be formed in pure-silica molecular sieves. In fact, we could not observe any noticeable ESR signals from dehydroxylated pure-silica ZSM-5 or SSZ-24.

Conclusions

ESR spectroscopy has been used to investigate paramagnetic defect centers in aluminophosphate ($AlPO_4$) molecular sieves with different structures dehydroxylated under 10^{-5} Torr at 773 K. It is observed that the nature and amount of paramagnetic defect centers formed in $AlPO_4$ molecular sieves depend highly on the structure type of the molecular sieves and their synthesis method. In particular, the spin concentration of paramagnetic

defects per unit cell of the molecular sieve increases as the ring size of the molecular sieve is larger. The ESR results obtained from SAPO and CoAPO molecular sieves reveal that the formation of paramagnetic defect centers is significantly restricted by increasing the amount of heteroatoms present in the framework. The proposed mechanism of formation of paramagnetic defect centers in $AlPO_4$ molecular sieves is in agreement with the overall ESR results obtained from this study. We hope that the unique ability of the $AlPO_4$ molecular sieves to produce paramagnetic defect centers in a dehydroxylated state will increase their applications as catalysts and separation media.

Acknowledgment. We thank Prof. R. Ryoo of the Chemistry Department at KAIST for his help in collecting the ^{29}Si MAS NMR spectra. This work was supported by the Korea Institute of Science and Technology under the contract Nos. 2N13723 and 2E14110.

JA960419I